Brain-Machine Interface for Mechanical Ventilation Using Respiratory-Related Evoked Potential

Sylvain Chevallier, Guillaume Bao, Mayssa Hammami, Fabienne Marlats, Louis Mayaud, Djillali Annane, Frédéric Lofaso, Eric Azabou

Brain-Machine Interface for Mechanical Ventilation Using Respiratory-Related Evoked Potential

Sylvain Chevallier[1(✉)] , Guillaume Bao[2], Mayssa Hammami[1],
Fabienne Marlats[1], Louis Mayaud[3], Djillali Annane[2], Frédéric Lofaso[2],
and Eric Azabou[2]

[1] LISV - University of Versailles St Quentin, Versailles, France
sylvain.chevallier@uvsq.fr
[2] Garches Neuro-Physio-Lab, Raymond Poincaré Hospital, AP-HP, Inserm 1173,
University of Versailles St Quentin, Versailles, France
eric.azabou@aphp.fr
[3] Mensia Technologies, SA, Paris, France

Abstract. The correct ventilation for patients in intensive care units plays a critical role for the prognostic and the recovery during the stay in the hospital. Desynchronization between the ventilator and the patient is an important source of stress, emphasized by the lack of communication due to intubation or loss of consciousness. This contribution proposes a novel approach based on electroencephalographic (EEG) activity to detect breathing effort. Relying both on recent neuroscience finding on respiratory-related evoked potential and on latest development of information geometry, the proposed approach elaborates on Riemannian distances between EEG covariance matrices to differentiate among different respiratory loads. The results demonstrate that this approach outperform existing state-of-the-art methods quantitatively, in terms of mean accuracy, and qualitatively, being able to predict level of breathing discomfort.

Keywords: Brain-machine interface · Electroencephalography
Riemannian geometry · Mechanical ventilation

1 Introduction

Brain-machine interfaces (BMI) allow to interact with a physical system using only cerebral activity and are mostly of interest in situations where muscle activity is not reliable or possible [24]. BMI also offer an opportunity for situations where communication is difficult: it is still possible to measure a brain response to specific stimulus or situation for unconscious patients [19]. Endotracheal ventilation ("intubation") is a commonly used intervention in the ICU [8] that impairs verbal communication. In this context a reliable objective assessment of ventilators performance is of particular importance both for patient's quality of

stay and clinical outcome. In the case of patient-ventilator asynchrony [6], the ventilator could interfere or impede the autonomous breathing function, which is an automatic and unconscious process, inducing dyspnea. The dyspnea, that is the sensation of shortness of breath, could be the cause of stressful experiences, with psychological or physical consequences [21].

To avoid these situations of asynchrony between a patient and the mechanical ventilation, they should be detected as soon as possible. Common approaches are relying on measurements of physiological signals, such as pressure, flow or blood oxygen saturation, and biosignals, such as electromyography. Several algorithms have been proposed to automatically detect these asynchrony, but they are restricted to certain types of disharmony [2,18]. The cortical networks for breathing control generate an activity observable on EEG [7] and the discomfort level have been reported to be correlated with this neural activity [13]. Two different kinds of neural activity are reported in the literature: preinspiratory potentials that are event-related desynchronization [7,10] and respiratory-related evoked potential which are event-related potential [13].

The detection and classification of these neural activity have been widely explored in the brain-machine interface community. The event-related desynchronization has been studied in the context of motor imagery-based paradigm and the event-related potentials are usually employed with oddball paradigm that elicits a P300 potential. Unfortunately, these signals are difficult to detect because of the poor signal-to-noise ratio and the variability of EEG signal from one subject to another. The most common approach is to design a patient-specific spatial filters to enhance the signal of interest and it is often associated with a reduction of dimensionality of the input. Unfortunately, these highly parametric approaches suffer from various levels of overfitting and underperform on new data [15]. Recent advances and a complete review could be found in [14].

Methods based on Riemannian geometry allows to revisit covariance-based algorithms by considering the spatial covariance matrices in an adequate space. Covariance matrices are symmetric and positive definite, they are elements of manifold with a negative curvature. Euclidean distance is not adequate on these manifolds; specific distances and divergences should be considered [12]. Riemannian methods achieve state-of-the-art results on multiple BCI paradigm, in depth reviews are provided in [4,25]. The study of [10,17] is the first attempt to use Riemannian geometry for the detection of respiratory states, based on preinspiratory potentials. The authors classify two situations, resting unloaded breathing and inspiratory threshold loading, with a variant of the Minimum Distance to Mean inspired by the k-mean algorithm.

The contributions described in this paper are the following:

– this is the first attempt to use Riemannian geometry on respiratory-related evoked potentials (RREP) instead of preinspiratory potentials (PIP),
– classification is done in the tangent space, whereas existing approach use a variation of a Riemannian k-mean,
– the experimental results goes beyond the binary classification (resting vs respiratory load) to perform a multiclass detection of the respiratory load,

– the obtained results outperform previously reported results, in a more challenging setup (multiclass instead of two classes).

The next section describes the existing approaches for detecting respiratory-related evoked potentials and preinspiratory potentials, along the proposed Riemannian framework. Section 3 provides the details concerning the experiment and the dataset. The described approaches are compared in Sect. 3.2 and the classification accuracy is estimated in different setups. These results are discussed in Sect. 4.

2   Methods

We will denote as $X \in \mathbb{R}^{C \times N}$ an EEG signal recorded with C electrodes during N time steps. This EEG signal corresponds to a session containing multiple trials.

2.1   Existing Approaches

When dealing with evoked potentials, XDAWN filters are a robust and widely employed algorithm [20]. It tries to uncover a stimulus $E \in \mathbb{R}^{N_t \times C}$, where N_t is number of time steps of the stimulus, by exploiting the temporal information of the session with $D \in \mathbb{R}^{N \times N_t}$, a Toeplitz matrix with 0 except for stimulus timing. Starting from the model that the EEG is $X^T = DE + \eta$, where $\eta \in \mathbb{R}^{C \times N}$ is non-target signal, the objective of XDAWN is to find a suitable spatial filter $W \in \mathbb{R}^{C \times N_f}$ that enhances the stimulus while reducing the non-target signal. N_f is the number of selected filters. The goal is to find W that maximizes the SSNR:

$$\hat{W} = \mathrm{argmax}_W \frac{\mathrm{tr}\ W^T \hat{\Sigma}_1 W}{\mathrm{tr}\ W^T \hat{\Sigma}_X W} \ , \tag{1}$$

with $\hat{\Sigma}_1 = \hat{E}^T D^T D \hat{E}$, $\hat{X}_X = XX^T$ and $\hat{E} = (D^T D)^{-1} D^T X^T$.

Similarly, for motor imagery, the most common preprocessing technique is to rely on Common Spatial Patterns (CSP) to filter the signal [3]. The EEG signal X should be centered and scaled and it is customary to bandpass filter the signal in the frequency of interest. After epoching the signal, two covariance matrices Σ_1 and Σ_2 are estimated, that correspond to 2 conditions. CSP is obtained by the simultaneous diagonalization of:

$$W^T \Sigma_1 W = \Delta_1 \text{ and } W^T \Sigma_2 W = \Delta_2, \text{ s.t. } \Delta_1 + \Delta_2 = I \tag{2}$$

The common practice is to select only a subset of spatial filters from W.

After this preprocessing, the data are usually well separated, thus a simple classifier such as Fisher Linear Discriminant Analysis is sufficient to achieve very high classification results. In this work, we also consider an SVM classifier using either linear or RBF kernel, chosing the hyperparameters via cross-validation. To ensure the reproducibility of the results and facilitate the comparison with [17],

we also consider the One-Class SVM [23] in our experiment. One should note that a direct comparison with [17] is not possible, their study is restricted to a two-class model and rely on AUC estimator whereas our study is multiclass and evaluate models through their accuracy. Accuracy is a basic but correct estimator in this context as the classes are balanced and the classifer are unbiaised [9].

2.2   Riemannian Geometry

Covariances matrices Σ are symmetric and positive-definite (SPD). Spatial covariance matrices could directly be estimated from multivariate EEG signals and we rely on a more robust estimator that sample covariance estimation $\hat{\Sigma} = \frac{1}{N} X X^T$, that is Schäfer-Strimmer estimator [11,22]. Covariance matrices capture well changes of amplitude characteristic of event-related desynchronization, but should be adapted to be suited to evoked potentials detection. So-called extended covariance matrices [5] incorporate evoked potential temple information, here we use XDAWN to build these extended covariance matrices. The covariance matrices are estimated from the extended signal $X_{\text{ext}} = \begin{bmatrix} E^T \\ X \end{bmatrix}$, $X_{\text{ext}} \in \mathbb{R}^{2C \times N_t}$.

It is possible to choose a metric such that the inner product on the tangent space $T_\Sigma \mathcal{M}$ of each point Σ varies smoothly from one point to another. In that case, all the points "glued" together are considered as a differentiable manifold $\mathcal{M}$. For the set of SPD matrices, one could choose the following inner product

$$\langle \Theta | \Theta' \rangle_\Sigma = \text{tr}(\Sigma^{-1} \Theta \Sigma^{-1} \Theta'),$$

for Θ and Θ' in $T_\Sigma \mathcal{M}$. This inner product allows to compute the path between any pair of points from $\mathcal{M}$, this path is called a curve and the shortest path between two points is a geodesic $\gamma(t)$. The length of the geodesic curve between Σ_1 and Σ_2 is the Riemannian distance δ:

$$\delta(\Sigma_1, \Sigma_2) = \left\| \log(\Sigma_1^{-\frac{1}{2}} \Sigma_2 \Sigma_1^{-\frac{1}{2}}) \right\|_F . \tag{3}$$

It is known as the affine-invariant Riemannian metric [16].

Any point Θ of the tangent space $T_\Sigma \mathcal{M}$ could be mapped on $\mathcal{M}$ with

$$\Sigma' = \exp_\Sigma(\Theta) = \Sigma^{\frac{1}{2}} \exp(\Sigma^{-\frac{1}{2}} \Theta \Sigma^{-\frac{1}{2}}) \Sigma^{\frac{1}{2}}$$

and the reverse mapping, from $\mathcal{M}$ to $T_\Sigma \mathcal{M}$ is

$$\Theta = \log_\Sigma(\Sigma') = \Sigma^{\frac{1}{2}} \log(\Sigma^{-\frac{1}{2}} \Sigma' \Sigma^{-\frac{1}{2}}) \Sigma^{\frac{1}{2}} .$$

The geodesic $\gamma(t)$ on the manifold could then be defined as:

$$\gamma(t) = \exp_{\Sigma_1}(t \log_{\Sigma_1}(\Sigma_2)) \tag{4}$$

Another important notion is the mean of Σ_i points, which is computed differently in the context of Riemannian manifold. This is the point minimizing the square of the distance between $\bar{\Sigma}$ and a Σ_i.

$$\bar{\Sigma} = \mathrm{argmin}_\Sigma \sum_{i=1}^{N} \delta^2(\Sigma_i, \Sigma). \tag{5}$$

In BMI, two approaches have been proposed for classification. The first one is simply a classification in the tangent space located at the Riemannian mean of the whole session [1]. The main interest of this approach is that all Euclidean algorithm (LDA, SVM and others) could be directly applied in this tangent space. It should be noted that elements of this space are symmetric matrices, thus the dimension of the input is $C(C+1)/2$ instead of C^2.

The other classifier is called *Minimum Distance to Mean* (MDM), introduced in [1], is presented for multi-class classification in the manifold. The classification is decided from the nearest class mean. One of the interest of this approach is that all the computation are made on the manifold, no computation take place on the tangent space.

3   Experiments

The study protocol was approved by the local Ethics committee (CPP): number 11073 on 2011-11-24, and is part of the trial registered in the public trials registry, http://clinicaltrials.gov, number NCT01548586. All study participants gave their informed, written consent.
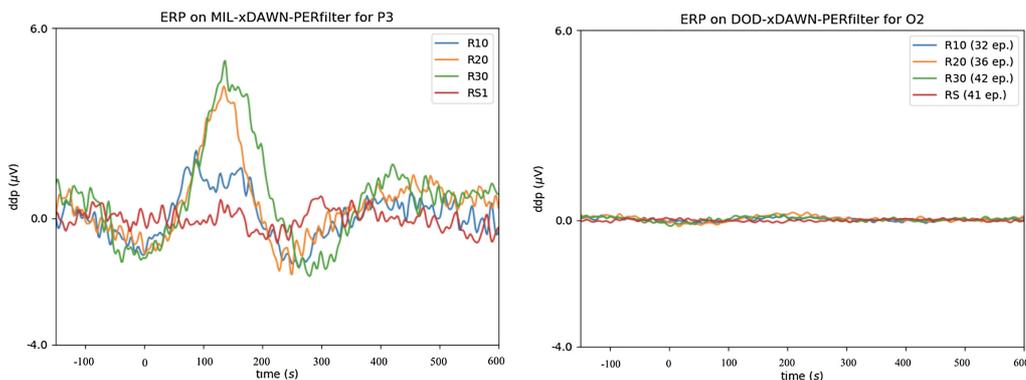

Fig. 1. Evoked potentials found for the subject with the best and the worst classification results, that is MIL and DOD subject. The RREP are filtered with XDAWN to using 8 components.

3.1 Setup and Dataset

The subject was seated comfortably and breathed into a mouthpiece connected to a low-resistance non-rebreathing valve (2600 Medium, Hans Rudolph Inc., St Louis, MO). Respiratory flows were recorded using a pneumotacho-Graph (Fleish no. 2, Lausanne, Switzerland) connected to a differential pressure transducer (TMSi 45 5cmH2O, Holland). Mouth pressure (MP) was measured using a differential pressure transducer (Validyne MP 45 100 cmH2O) and end-tidal pressure of CO2 (PETCO2) using a capnograph (Capnogard 1265, Novametrix, Wallingford, CT). EEG signal was recording synchronously with the breathing using a 19 electrodes Cap (EasyCap, Brain Products GmbH, Germany). Active electrodes were placed in equidistant positions (ActiCap, Brain Products GmbH, Germany) according to the conventional "10–20" topographic system. The ground electrode was positioned at AFz. The EEG signal was digitized at 2000 Hz and recorded using NeuroRT Studio (Mensiatech, Chantepie, France) for subsequent processing.

After an adaptation period during which the subjects breathed quietly through the unloaded circuit, the lowest and highest loads to be investigated were applied during a few respiratory cycles to familiarize the subjects with the load range and evaluation scale. The subjects were then exposed to five levels of inspiratory pressure load conditions (PEEP valve for vital flow 100 set; Vital Signs Inc., Gamida, France):

– Spontaneous breathing through the unloaded circuit (RS)
– Breathing with a resistive load of 10 cmH2O (R10),
– Breathing with a resistive load of 20 cmH2O (R20),
– Breathing with a resistive load of 30 cmH2O (R30).

Each load was applied for 5 min respiratory cycles, after a 3 min rest. To assess that the different loads are generating RREP, Fig. 1 shows the average evoked potentials obtained for each condition (RS, R10, R20 and R30) for two subjects, those with the best and the worst classification results.

3.2 Results

Five methods are evaluated on this dataset: MDM and Tangent Space classification, both introduced in Sect. 2.2, XDAWN+LDA as explained in Eq. (1), One-Class SVM operating on vectorized covariance matrices (SVMeeg), as proposed by [17] and a linear SVM (SVMphy) operating input vectors of 6 features from the MP sensors (peak, average, total volume, flow variance, skewness and kurtosis) [17]. An extensive recursive feature selection process is set up for selecting the best features among the 2^6 possibility for SVMphy classifier. All the methods are evaluated through 10-fold validation using accuracy, as the classes are balanced and the classifer are unbiaised [9].

Figure 2 shows the obtained accuracy for all subjects in the multiclass case. Classification in the tangent space offers the best results and outperform all other methods for all subjects. The second method is the SVM based on physiological

parameters which achieves honorable results. The XDAWN+LDA and the MDM classifiers yield comparable results, the MDM displaying a larger variance. The SVM classifying the covariance matrices is performing very poorly, confirming that Euclidean approaches are not suited to deal correctly with curved manifold.
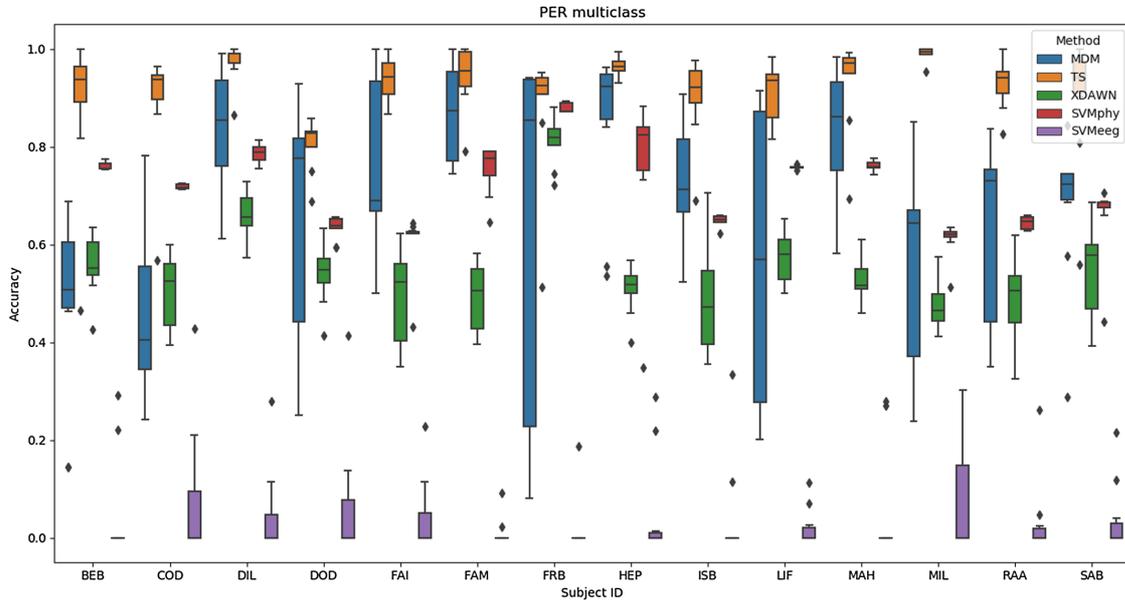

Fig. 2. Comparison of multiclass detection of RREP for each of the 14 subjects with Riemannian approaches Minimum Distance to Mean (MDM) and Tangent Space (TS) and state of the art approaches, that is XDAWN+LDA and SVM based on physiological (SVMphy) or EEG inputs (SVMeeg).

Table 1. Accuracy values for binary classification, that is detection of normal breathing vs respiratory load. The accuracies are compared for the proposed Riemannian approach (Tangent Space on EEG) for both evoked potential (RREP) and pre-inspiratory potential (PIP), and for state-of-the-art approach for physiological input (SVM on pressure sensors).

Method	Input	Accuracy (%)
SVM physiological data	RREP	$71.76 \pm 9.83\%$
Tangent space	**RREP**	**$93.46 \pm 10.04\%$**
SVM physiological data	PIP	$85.17 \pm 12.85\%$
Tangent space	PIP	$87.75 \pm 12.72\%$

Figure 3 shows the average accuracy values for the multiclass case (discriminating between RS, R10, R20 and R30) and the two-class case (RS vs R10/R20/R30). The two-class case allows a comparison with the state-of-the-art study of [17]: it could be seen that the results of all the methods are slightly

degraded in the multiclass case. Table 1 summarizes the results of the two-class case with RREP and compares with the two best methods for PIP. Tangent space classification on RREP obtains the best results.
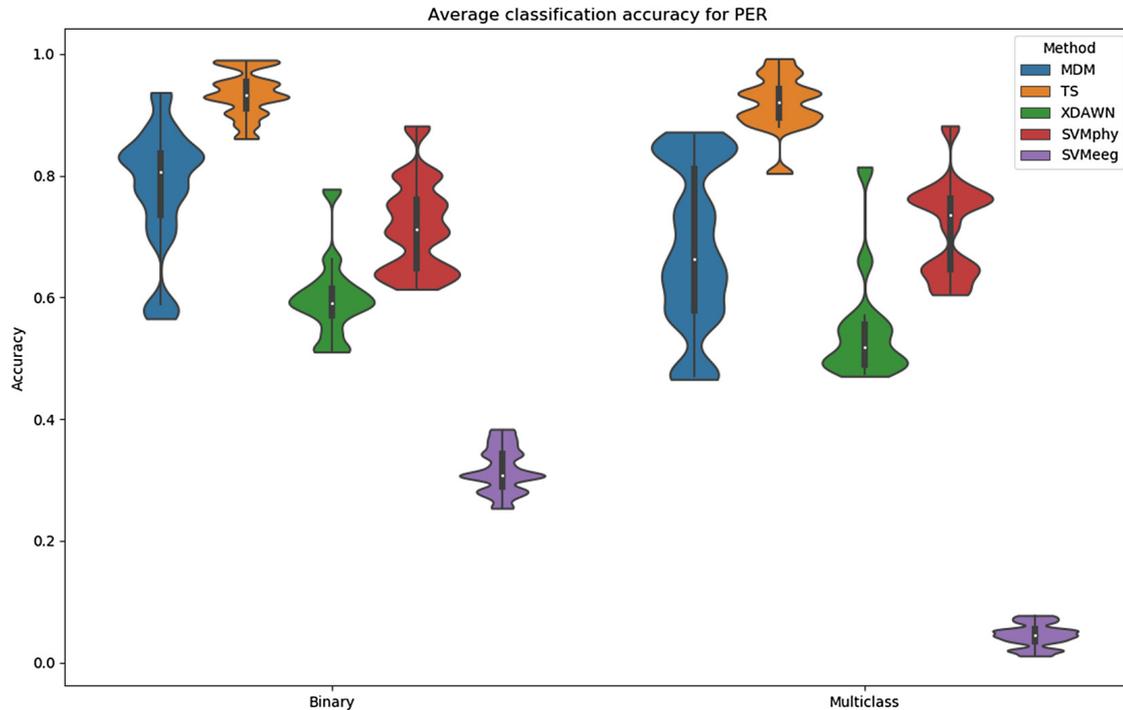

Fig. 3. Mean values for RREP classification for all subjects under 3 increasing respiratory loads and one control condition, for MDM, Tangent Space, XDAWN+LDA, SVM based on physiological and EEG data.

4 Discussion and Conclusion

This paper presents a first step towards a closed-loop BMI ventilator. One current limitation is that EEG is expensive, cumbersome, sensitive to various sources of noise, and not suitable for long-term recordings. Nonetheless, these limitations could be mitigated in a medical and controlled environment. For online processing, the proposed method still needs a physiological channel to extract cues for inspiration and expiration. This drawback is of limited importance as such sensors are cheap and already available on existing ventilator devices.

The existing approaches are relying on physiological or behavioral information, but lack precision to detect certain asynchronous state. A first attempt to use EEG information together with Riemannian geometry yield promising results, but the method proposed by the authors require to tune several parameters and is limited to a two-class case.

The proposed method relies on respiration-related evoked potentials instead of pre-inspiratory potentials and thanks to an appropriate Riemannian classifier outperforms current state of the art. The results are more accurate and allow to detect different respiratory loads, and thus open the possibility quantify the breathing effort.

References

1. Barachant, A., Bonnet, S., Congedo, M., Jutten, C.: Multiclass brain-computer interface classification by Riemannian geometry. IEEE Trans. Biomed. Eng. **59**(4), 920–928 (2012)
2. Blanch, L., et al.: Validation of the better care® system to detect ineffective efforts during expiration in mechanically ventilated patients: a pilot study. Intensiv. Care Med. **38**(5), 772–780 (2012)
3. Blankertz, B., Tomioka, R., Lemm, S., Kawanabe, M., Muller, K.R.: Optimizing spatial filters for robust EEG single-trial analysis. IEEE Signal Process. Mag. **25**(1), 41–56 (2008)
4. Congedo, M., Barachant, A., Bhatia, R.: Riemannian geometry for EEG-based brain-computer interfaces; a primer and a review. Brain-Comput. Interfaces **4**, 1–20 (2017)
5. Congedo, M., Barachant, A., Andreev, A.: A new generation of brain-computer interface based on Riemannian geometry. arXiv preprint arXiv:1310.8115 (2013)
6. Dres, M., Rittayamai, N., Brochard, L.: Monitoring patient-ventilator asynchrony. Curr. Opin. Crit. Care **22**(3), 246–253 (2016)
7. Dubois, M., et al.: Neurophysiological evidence for a cortical contribution to the wakefulness-related drive to breathe explaining hypocapnia-resistant ventilation in humans. J. Neurosci. **36**(41), 10673–10682 (2016)
8. Esteban, A., et al.: How is mechanical ventilation employed in the intensive care unit? An international utilization review. Am. J. Respir. Crit. Care Med. **161**(5), 1450–1458 (2000)
9. Fatourechi, M., Ward, R.K., Mason, S.G., Huggins, J., Schlögl, A., Birch, G.E.: Comparison of evaluation metrics in classification applications with imbalanced datasets. In: International Conference on Machine Learning and Applications (ICMLA), pp. 777–782. IEEE (2008)
10. Hudson, A.L., et al.: Electroencephalographic detection of respiratory-related cortical activity in humans: from event-related approaches to continuous connectivity evaluation. J. Neurophysiol. **115**(4), 2214–2223 (2016)
11. Kalunga, E.K., Chevallier, S., Barthélemy, Q., Djouani, K., Monacelli, E., Hamam, Y.: Online SSVEP-based BCI using riemannian geometry. Neurocomputing **191**, 55–68 (2016)
12. Kalunga, E.K., Chevallier, S., Barthélemy, Q., Djouani, K., Hamam, Y., Monacelli, E.: From euclidean to riemannian means: information geometry for SSVEP classification. In: Nielsen, F., Barbaresco, F. (eds.) GSI 2015. LNCS, vol. 9389, pp. 595–604. Springer, Cham (2015). https://doi.org/10.1007/978-3-319-25040-3_64
13. Knafelc, M., Davenport, P.W.: Relationship between magnitude estimation of resistive loads, inspiratory pressures, and the rrep p1 peak. J. Appl. Physiol. **87**(2), 516–522 (1999)
14. Lotte, F., et al.: A review of classification algorithms for eeg-based brain-computer interfaces: a 10 year update. J. Neural Eng. **15**(3), 031005 (2018). http://stacks.iop.org/1741-2552/15/i=3/a=031005

15. Mayaud, L., et al.: Brain-computer interface for the communication of acute patients: a feasibility study and a randomized controlled trial comparing performance with healthy participants and a traditional assistive device. Brain-Comput. Interfaces **3**(4), 197–215 (2016)
16. Moakher, M.: A differential geometric approach to the geometric mean of symmetric positive-definite matrices. SIAM J. Matrix Anal. Appl. **26**(3), 735–747 (2005)
17. Navarro-Sune, X., et al.: Riemannian geometry applied to detection of respiratory states from EEG signals: the basis for a brain-ventilator interface. IEEE Trans. Biomed. Eng. **64**(5), 1138–1148 (2017)
18. Piquilloud, L., et al.: Neurally adjusted ventilatory assist (NAVA) improves patient-ventilator interaction during non-invasive ventilation delivered by face mask. Intensiv. Care Med. **38**(10), 1624–1631 (2012)
19. Reuter, B., Linke, D., Kurthen, M.: Cognitive processes in unconscious patients? A brain mapping study of the p300 potential. Archiv fur Psychologie **141**(3), 155–173 (1989)
20. Rivet, B., Souloumiac, A., Attina, V., Gibert, G.: xDAWN algorithm to enhance evoked potentials: application to brain-computer interface. IEEE Trans. Biomed. Eng. **56**(8), 2035–2043 (2009)
21. Rotondi, A.J., et al.: Patients' recollections of stressful experiences while receiving prolonged mechanical ventilation in an intensive care unit. Critical Care Med. **30**(4), 746–752 (2002)
22. Schäfer, J., Strimmer, K.: A shrinkage approach to large-scale covariance matrix estimation and implications for functional genomics. Stat. Appl. Genet. Mol. Biol. **4**(1) (2005)
23. Scholkopf, B., Smola, A.J.: Learning with Kernels: Support Vector Machines, Regularization, Optimization, and Beyond. MIT Press, Cambridge (2001)
24. Wolpaw, J., Birbaumer, N., McFarland, D.J., Pfurtscheller, G., Vaughan, T.M.: Brain-computer interfaces for communication and control. Clin. Neurophysiol. **113**(6), 767–791 (2002)
25. Yger, F., Berar, M., Lotte, F.: Riemannian approaches in brain-computer interfaces: a review. IEEE Trans. Neural. Syst. Rehabil. Eng. **25**(10), 1753–1762 (2017)